Far-IR SED-Fitting & CO Abundances of Massive Molecular Clumps in the CHaMP Survey

Rebecca L. Pitts[1], Peter J. Barnes[1,2], Stuart D. Ryder[3], Dan Li[4], Frank Varosi[1]

[1]University of Florida, USA; [2]University of New England, Australia; [3]Australian Astronomical Observatory; [4]National Optical Astronomy Observatory, AZ, USA

Abstract: We used FIR/sub-mm photometry from the Herschel Space Observatory[9,19] and the Atacama Pathfinder EXperiment (APEX, [21]) to fit pixel-by-pixel modified Planck SEDs[11] to molecular clumps in the Census of High- and Medium mass Protostars (CHaMP, [1,2,3]) (280°<l<300°, -4°<b<2°). We present maps of H_2 column density for molecular clumps in the Carina Nebula complex (Regions 9 - 11), and surrounding RCW 64 (Region 26). We compare the column densities of CO and H_2 (N_{CO} and N_{H2}) to chart spatial variations in their correspondence, and derive maps of the CO abundance (denoted [CO/H_2]). We find the CO abundance varies by an order of magnitude or more across each region, averaging a few$\times10^{-5}$ per H_2, and its distribution across each clump correlates with environmental conditions, especially dust temperature. This, plus the tension between dust- and CO-derived H_2 column densities shows that even at clump scales, no one CO abundance is appropriate to convert from N_{CO} to N_{H2}. We also find that L/M from dust continuum SED-fitting depends almost exclusively on dust temperature and thus does not independently trace cloud evolution. Finally, using data from the Australia Telescope Compact Array (ATCA*) and Gemini's Thermal-Region Camera Spectrograph (T-ReCS, [22]) to de-blend BYF73 (in Region 9) in the FIR/submm, we find protostellar objects account for <3% of its mass. BYF73's most massive core, MIR 2, accounts for ~1% of the clump's 2×10^4 $M_\odot$ mass but nearly half of its ~$10^4 L_\odot$ luminosity.

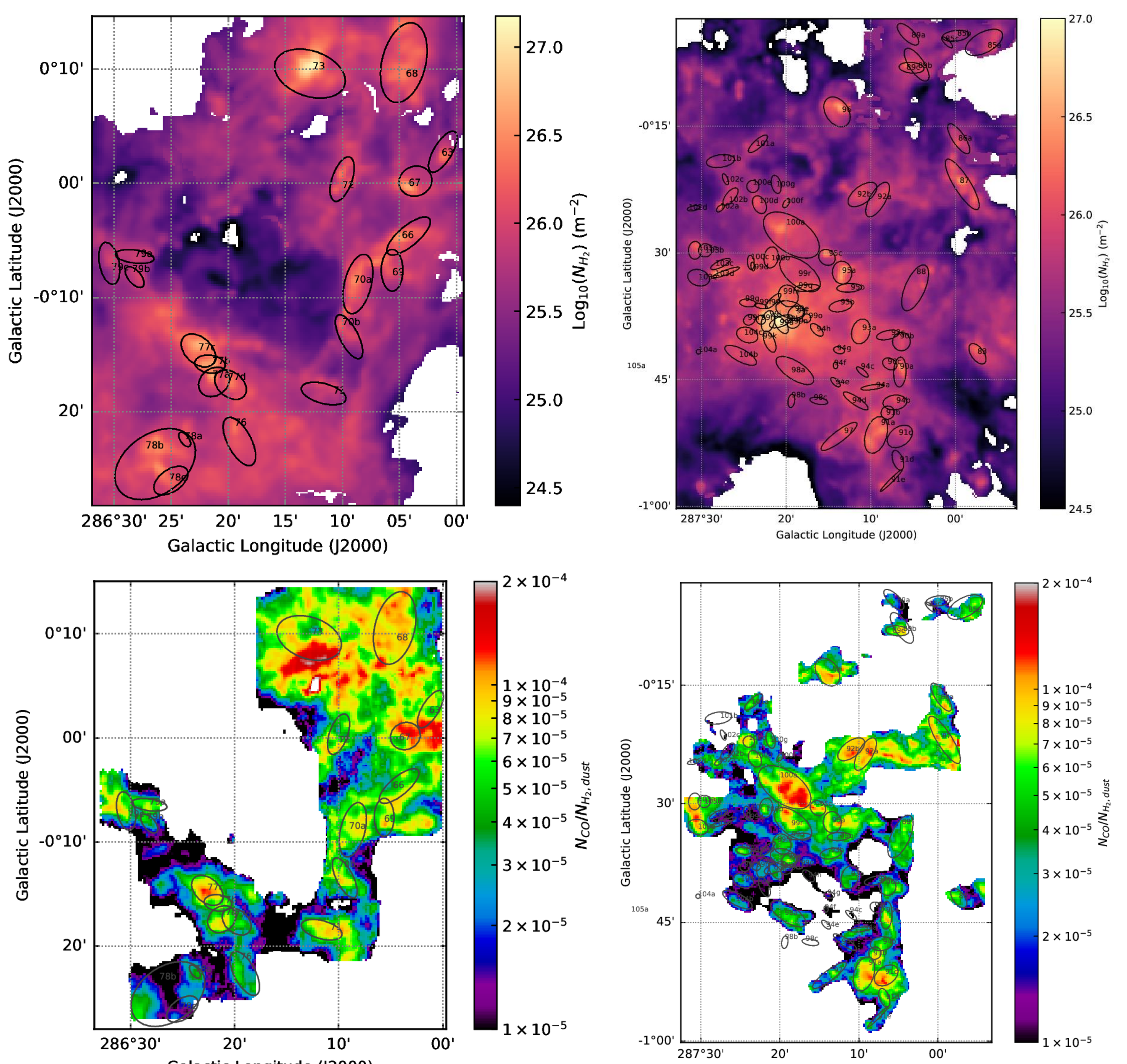

N_{H2} (pink) and CO abundance (rainbow) maps of Regions 9 (*above left column*), 10 (*above right column*), and 26b (*below*). Regions 11 and 26a are not shown, but have similar ranges of values to Regions 10 and 26b respectively. Note the poor correspondence between the peaks in N_{H2} and those in [CO/H_2]

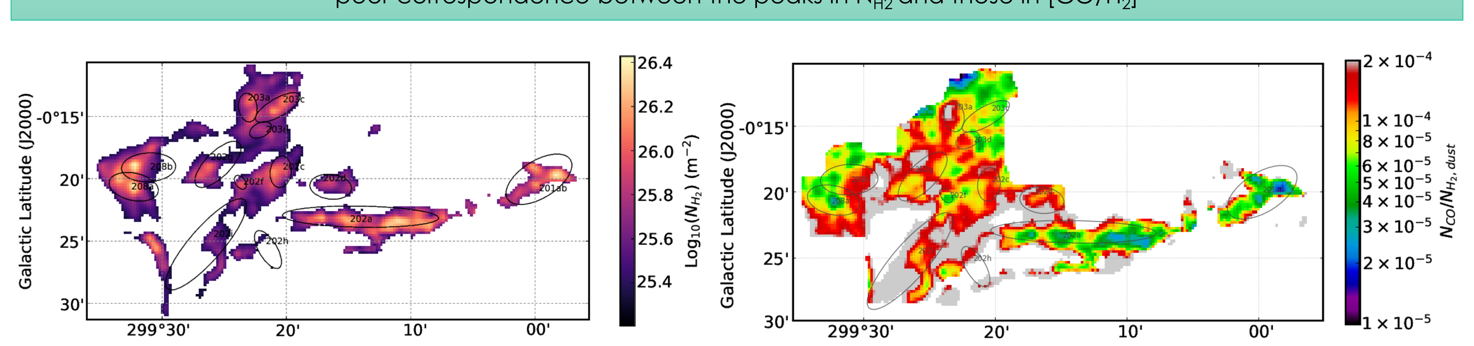

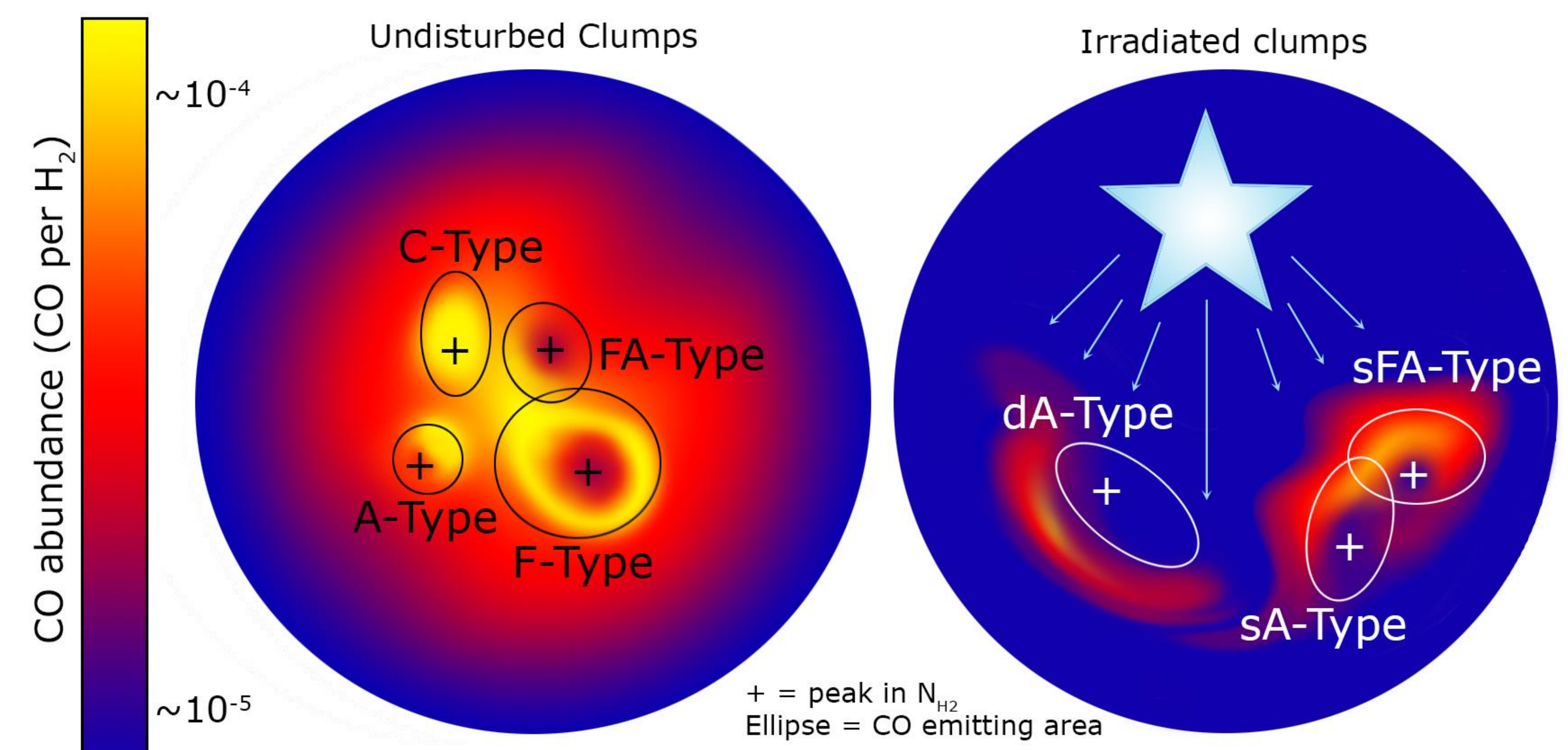

Types		Sub-types
C = Coincident	A = Asymmetric	d = dissociating
F = Frozen-out	FA = F/A hybrid	s = sublimating

CO Abundance: appearance is physics and environment matters[18]

To compute CO abundance, we divided N_{CO} maps from Barnes+2018 by dust-based N_{H2} maps. Comparing to the N_{H2} maps, and knowing the locations of nearby OB stars/clusters, each clump could be classed by appearance in [CO/H_2] as:

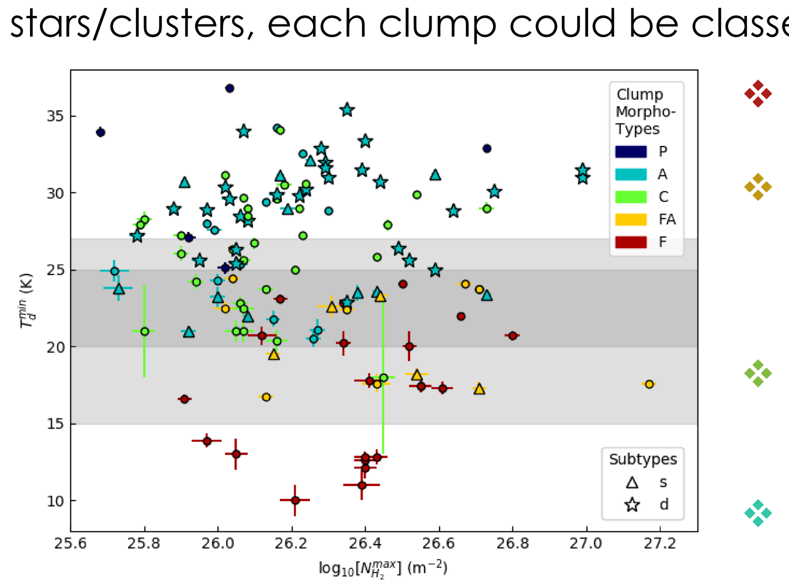

Type (*Subtype*)	Count	$\langle T_d^{min} \rangle$ (K)	$\langle \sigma_T \rangle$ (K)
P	5	33	6
A	55	29	4
sA	*12*	*27*	*4*
dA	*30*	*30*	*3*
C	30	28	5
FA	15	22	3
sFA	*5*	*20*	*3*
F	21	18	5
Total	126	27	7

- **F-Type:** local **maximum** in N_{H2} coincides with local **minimum** in [CO/H_2]
- **FA-Type:** same as F-Type, but higher-[CO/H_2] envelope is lop-sided. If the highest-[CO/H_2] side faces an ionizing radiation source, it is a *Sublimating FA (sFA)-Type*.
- **C-Type:** local **maximum** in N_{H2} coincides with either a local **maximum** in [CO/H_2] or a flat [CO/H_2] distribution.
- **A-Type:** local **maxima** in N_{H2} and [CO/H_2] are offset from each other. If a known OB star/cluster is nearby, these may be subdivided as:
  - **Sublimating (sA-Type):** where [CO/H_2] enhancement faces an ionizing flux source.
  - **Dissociating (dA-Type):** where [CO/H_2] peaks opposite the local max in N_{H2} from the ionizing flux source. Max [CO/H_2] is often very low.
- **P-Type:** local maximum in [CO/H_2] has no counterpart in N_{H2}; usually tiny.

These morphologies were found to correlate with the minimum temperature of the clump in a way that, unlike N_{H2}, was not vastly different from cloud to cloud.

On a pixel-by-pixel basis, [CO/H_2] vs. dust temperature is a snapshot of the competition between CO desorption from ice and CO dissociation. There exists a temperature between ~15 and 27 K where the pixel-averaged [CO/H_2] is maximized near the canonical 10^{-4} [4-7,13,15-17], and almost any clump morphotype can be seen. CO ice binding energy increases with the temperature at which it froze out [15-17], so the temperature of maximal [CO/H_2] encodes information about the cloud's earliest physical conditions.

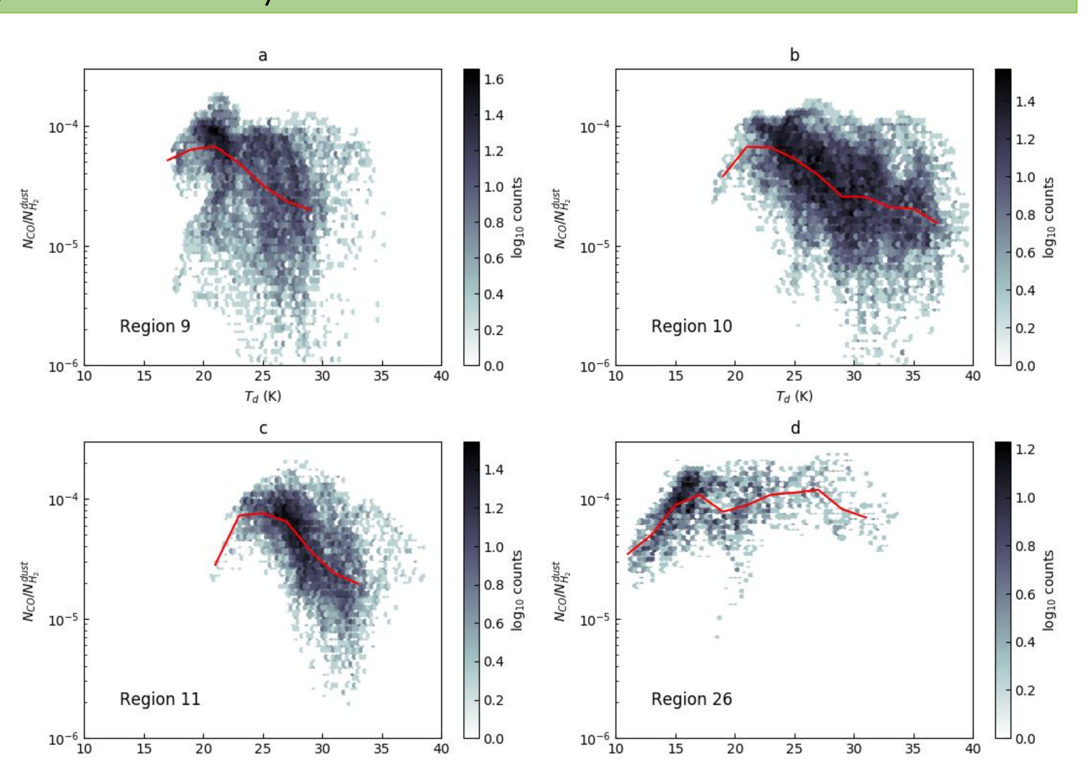

L/M from dust SED-fitting traces temperature, not evolution

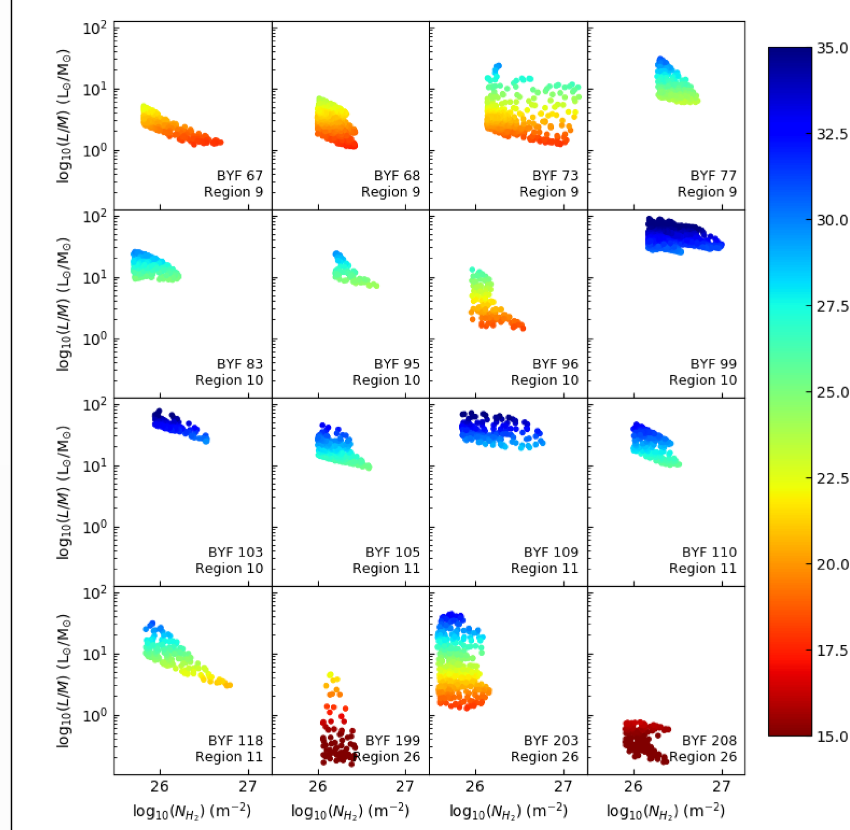

In the optically thin limit, the dependence of L/M on N_{H2} disappears, so if the dust emissivity index (β), dust opacity coefficient (κ_0), and gas-to-dust ratio (γ) are held constant, L/M becomes an abstract restatement of the temperature:

$$\frac{L/M}{L_\odot/M_\odot} \approx \frac{4\pi}{\cancel{N_{H_2}\mu m_H}} \int_0^\infty \left(\frac{\cancel{N_{H_2}\mu m_H}\kappa_0}{\gamma}\right)\left(\frac{\nu}{\nu_0}\right)^\beta B_\nu(T)d\nu = \frac{4\pi\kappa_0 h}{c^2\gamma\nu_0^\beta}\left(\frac{kT}{h}\right)^{\beta+4}\Gamma(\beta+4)\zeta(\beta+4)$$

L/M does, however, make visible the exceptionally weak inverse correlation between N_{H2} and T in starless clumps. Only clumps known to contain protostars have a different functional form.

Case Study: BYF 73 is one of the least-evolved massive molecular clumps known

Top: [OI]145/[CII]158 line ratio map via FIFI-LS.
Bottom: 3-color Herschel image (70, 160, & 350 μm)

T-ReCS resolved 8 MIR sources at 8.74, 10.4, 12.3, and 18.3 μm. Only MIR-1, 2, and 5 appear to be embedded, with A_V ranging from 15 to 55. Gaussian fitting to Herschel data at the known coordinates and PSFs recovered MIR 2 and 1. Our SED-fitting code was able to fit MIR 2 with T=49.2±0.5 K and N_{H2} = 8±1×10^{28} m^{-2}. If MIR-2's size at 3 mm is representative, its mass is thus 220±40 $M_\odot$ and its mean density n=8×10^{13} m^{-3}. This agrees with n from the ratio of the [OI] 145μm and [CII] 158μm lines, as well as the [CII] line flux, taken by FIFI-LS[8] aboard SOFIA and compared to n vs. FUV field strength (G) maps from PDR Toolbox[12]. The same maps constrain G along the PDR front west of BYF 73 to between $10^{1.5}$ and 10^2 G_0.

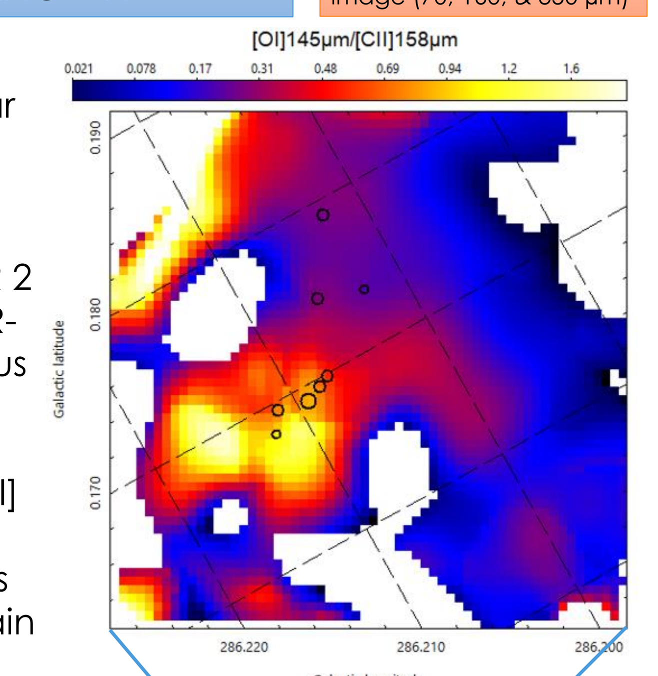

These measures also imply that using the depth of the 9.7μm silicate absorption line and $A_V/\tau_{9.7}$ = 18.5±0.1 mag[13] we may under-estimate the mass in dense gas by 100-fold or more.

MIR2 dwarfs MIR1 and 3, and pumps out ~50% (4770±40 $L_\odot$)of BYF73's total luminosity, but is only ~1% (220±40 $M_\odot$) of the total mass of the clump. Therefore, BYF 73 is ≳97% gas, one of the most gas-dominated star-forming clumps ever found. MIR 1-3 also show no signs of outflows at these sensitivities, so the physical conditions at the onset of massive star formation should be well-preserved. Thus BYF73 is among the most promising places to observe the elusive transition from starless core to class-0 protostar.

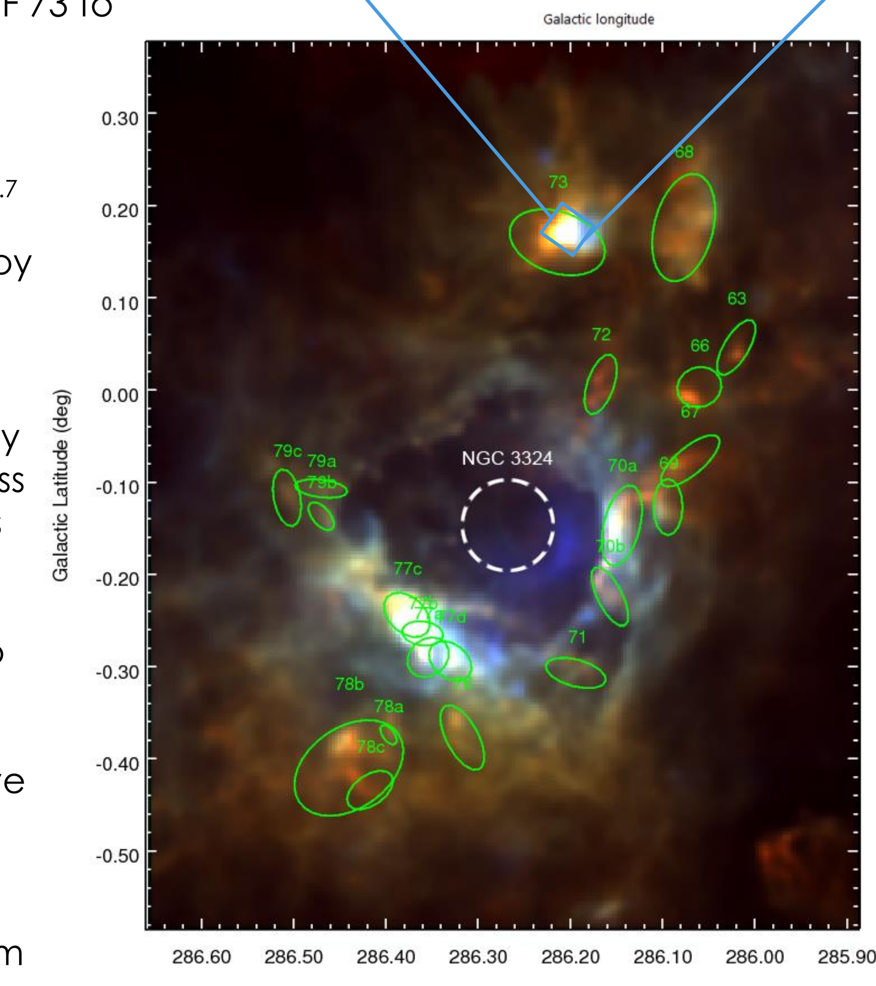

Papers and Supporting References

Pitts, R. L., Barnes, P. J., & Varosi, F., 2018, MNRAS, subm.
Pitts, R. L., Barnes, P. J., Ryder, S., Li, D., 2018, in prep.
[1] *Barnes P. J., Hernandez A. K., Muller E., Pitts R. L., 2018, ApJ, accepted[13]*
[2] *Barnes P. J., Ryder S. D., O'Dougherty S. N., et al., 2013, MNRAS, 432, 2231*
[3] *Barnes P. J., Muller E., Indermuehle B., et al., 2016, ApJ, 831, 67*
[4] Bacmann A., Lefloch B., Ceccarelli C., et al., 2002, A&A, 389, L6
[5] Beckwith S. V. W., Sargent A. I., Chini R. S., Guesten R., 1990, AJ, 99, 924
[6] Caselli P., Walmsley C. M., Tafalla M., et al., 1999, ApJ,523, L165
[7] Cazaux S., Martín-Doménech R., Chen Y. J., et al., 2017, ApJ, 849, 80
[8] Colditz, S., Fumi, F., Geis, N., et al., 2012, Proc. SPIE, 8446, 844617
[9] Griffin M. J., et al., 2010, A&A, 518, L3
[10] Hernandez A. K., Tan J. C., Caselli P., et al., 2011, ApJ, 738, 11
[11] Hildebrand R. H., 1983, Quarterly Journal of the Royal Astronomical Society, 24, 267
[12] Kaufman, M.J., Wolfire, M.G., & Hollenbach, D.J. 2006, ApJ, 644, 283
[13] Kramer C., Alves J., Lada C. J., et al., 1999, A&A, 342, 257
[14] Mathis, J.S. 1990, Annual Reviews of Astronomy & Astrophysics, 28, 37%--70
[15] Muñoz Caro G. M., Jiménez-Escobar A., Martín-Gago J. Á., et al., 2010, A&A,522, A108
[16] Muñoz Caro G. M., Chen Y. J., Aparicio S., et al., 2016, A&A, 589, A19
[17] Öberg K. I., van Dishoeck E. F., & Linnartz H., 2009, A&A, 496, 281
[18] Peñaloza C. H., Clark P. C., Glover S. C. O., et al., 2018, MNRAS,475, 1508
[19] Poglitsch A., et al., 2010, A&A, 518, L2
[20] Reach W. T., Heiles C., Bernard J. P., 2015, ApJ, 811, 118
[21] Siringo G., et al., 2009, A&A, 497, 945
[22] Telesco, C. M., Pina, R. K, Hanna, K. T., et al.,1998, Proc. SPIE, Vol. 3354, Infrared Astronomical Instrumentation, ed. Fowler, A.M, 534-544

*The Australia Telescope Compact Array is funded by the Commonwealth of Australia for operation as a National Facility managed by CSIRO.